



Co-funded by  
the European Union

## **EXSOLUTION-BASED NANOPARTICLES FOR LOWEST COST GREEN HYDROGEN VIA ELECTROLYSIS**



**CCD approach that combines Zirfon with exsolution catalyst from  
WP1 (Deliverable D3.2)**

The project is supported by the Clean Hydrogen Partnership and its members	
PU	Public, fully open <input checked="" type="checkbox"/>
SEN	Sensitive, limited under the conditions of the Grant Agreement <input type="checkbox"/>
Classified R- UE/EU-R	EU RESTRICTED under the Commission Decision No2015/444 <input type="checkbox"/>
Classified C- UE/EU-C	EU CONFIDENTIAL under the Commission Decision No2015/444 <input type="checkbox"/>
Classified S- UE/EU-S	EU SECRET under the Commission Decision No2015/444 <input type="checkbox"/>

*Co-funded by the European Union. Views and opinions expressed are however those of the author(s) only and do not necessarily reflect those of the European Union or Clean Hydrogen JU. Neither the European Union nor the granting authority can be held responsible for them.*

## NOTICES

---

For information, please contact the project coordinator, Elo Meier, e-mail: [elo.meier@stargatehydrogen.com](mailto:elo.meier@stargatehydrogen.com). This document is intended to fulfil the contractual obligations of the EXSOTHyC project, which has received funding from the Clean Hydrogen Partnership and its members, concerning deliverable D3.1 described in contract 101137604.

All intellectual property rights are owned by EXSOTHyC consortium and are protected by the applicable laws. Except where otherwise specified, all document contents are: “©EXSOTHyC Project - All rights reserved”.

Reproduction is not authorized without prior written agreement. The commercial use of any information contained in this document may require a license from the owner of that information. EXSOTHyC consortium is also committed to publish accurate and up to date information and take the greatest care to do so. However, EXSOTHyC consortium cannot accept liability for any inaccuracies or omissions nor accept liability for any direct, indirect, special, consequential, or other losses or damages of any kind arising out of the use of this information.

---

## Authors

---

Maximilian Demnitz, TU/e

---

## Reviewer(s)

---

Stefan Loos, IFAM

---

## Table of revisions

---

Version	Date	Description and reason	Author	Affected sections
v1.0	19 <sup>th</sup> March 2025	1 <sup>st</sup> revision of the draft	Stefan Loos	1-4
V2.0	20 <sup>th</sup> March 2025	Final version	Maximilian Demnitz, Stefan Loos	1-4

---

## List of Partners

---

Stargate Hydrogen Solutions OÜ (Stargate)

University of St Andrews (St Andrews)

Agfa-Gevaert NV (AGFA)

Eindhoven University of Technology (TUE)

Fraunhofer IFAM (IFAM)

---

## List of Abbreviations

---

AEM – anion exchange membrane  
HER – hydrogen evolution reaction  
HOR – hydrogen oxidation reaction  
HTO – hydrogen to oxygen crossover  
ISM – ion solvating membrane  
OER – oxygen evolution reaction  
ORR – oxygen reduction reaction  
OTH – oxygen to hydrogen crossover  
PGM – Platinum Group Metals  
Ra-Ni – Raney-Nickel  
RC – recombination catalyst

## List of Figures

---

Figure 1. Scheme showing the stencil coating procedure for making catalyst coated diaphragms.	8
Figure 2. 3D printed polypropylene flow cell used for temperature dependent experiments with forced flow. Not seen in this figure is the diaphragm, which is sandwiched between the two EPDM gaskets.	9
Figure 3. Polarization curves of pristine Zirfon with Ni felts, exsolution CCDs, and a conventional CCD. The measurements were conducted in 30 wt.% KOH with 50 $\mu$ M electrolyte Fe.	10
Figure 4. Internal resistance corrected polarization curves of pristine Zirfon with Ni felts, exsolution CCDs, and a conventional CCD. The measurements were conducted in 30 wt.% KOH with 50 $\mu$ M electrolyte Fe.	11
Figure 5. SEM images of the exsolution catalyst (Co-doped titanate) combined with graphitized carbon at varying resolutions. The table gives information about the elemental composition derived from EDX measurements.	12
Figure 6. TEM images of Co-doped titanate and Fe,Co-doped aluminate showing exsolution on the surface.	13

---

## Table of Contents

---

NOTICES.....	2
Authors .....	3
Reviewer(s) .....	3
Table of revisions.....	3
List of Partners .....	4
List of Abbreviations .....	5
List of Figures .....	6
1    Objectives.....	8
2    Methodology and Work done.....	8
3    Deviations.....	13
4    Conclusions .....	13

## 1 Objectives

Deliverable 3.2 aims to combine the usage of catalyst coated diaphragms with the novel developed catalyst from EXSOTHyC Work Package 1. The goal of the work is to achieve electrochemical performances that are even better than the CCDs prepared with conventional catalysts used in D3.1 “CCD approach for Zirfon material with optimal binder/catalyst choice, serving as benchmark CCD”. The performance of the exsolution CCDs should then be compared with the performance of CCS made with exsolution catalysts.

## 2 Methodology and Work done

The preparation of CCDs based on catalyst powders with exsolved particles followed a similar procedure employed in D3.1.

For stencil coating PVA was first dissolved in deionized water (100 g/L) at 100 °C for at least 12 h hours. For the stencil coating procedure 100 mg of catalyst was first added to a glass vial into which 1 g of water with 10 mg PVA was added. Two exsolution based catalysts were used, one targeted for HER (Fe, Co-doped aluminate) and one for OER (Co-doped titanate). For each catalyst a separate ink was prepared.

To try and further enhance the conductivity of the CCD, a second set of inks was made, where additionally 200 mg of carbon black was added for both inks. The ink was then ultrasonicated for one hour and placed with a dispensable pipette on a stencil coating template. The thick slurry ink was then drawn with a sharpened metal squeegee over the 100 µm thick template, which has an exposed coating area (see Figure 1).

Afterwards the CCD was dried for several hours at room temperature in a vacuum oven. The loading per side was determined by measuring the weight of the diaphragm before and after the coating and dividing the mass by coating area (2.85 cm<sup>2</sup>).

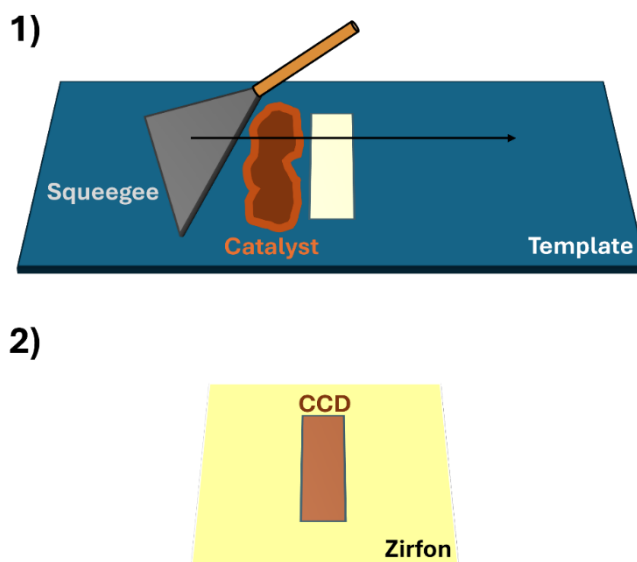


Figure 1. Scheme showing the stencil coating procedure for making catalyst coated diaphragms.

A 3D printed polypropylene flow cell (in-house design; see

Figure 2) was used for electrochemical performance tests of the CCDs. They were placed in the center of the cell and sandwiched from both sides using 200  $\mu\text{m}$  thick Ni felts (Bekaert CURRENTOR® 2NI06-0.20,  $A_{\text{geom}} = 0.95 \times 3.00 = 2.85 \text{ cm}^2$ ) that functioned as porous transport layers (PTLs). The current was transported to the PTLs via perforated Ni plates that were in contact with stainless steel screws. Into the screws the banana plugs connecting the potentiostat were inserted. The zero-gap cell was pressed together using screws onto which a torque of 2.5 N·m was applied. As a potentiostat a Vertex 10A (Ivium Technologies) was used and connected to the cell in a 4-terminal connection.

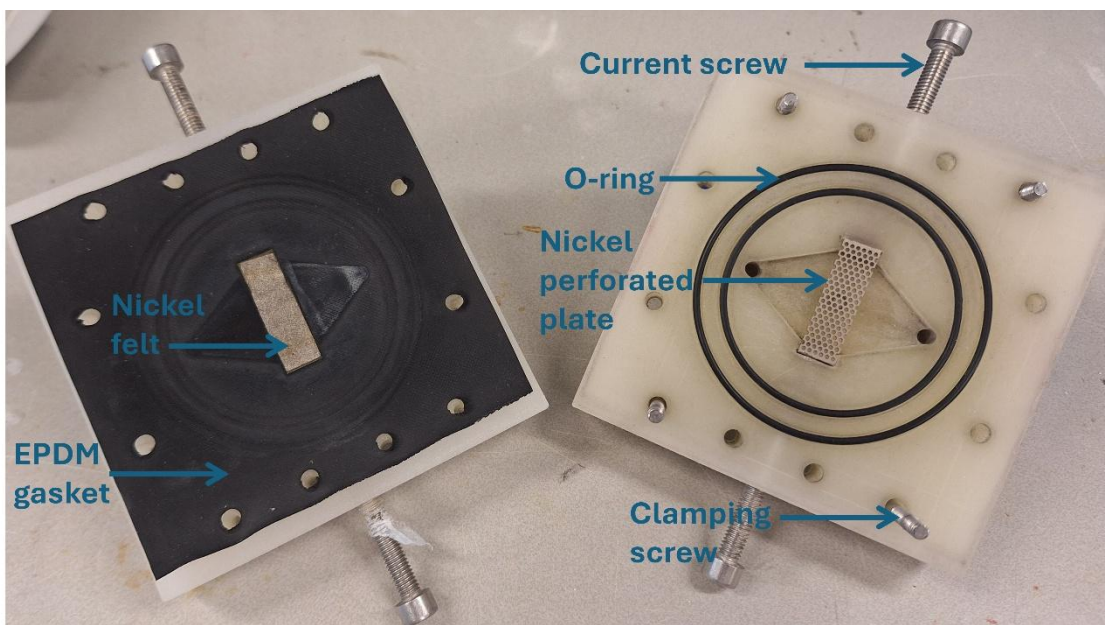


Figure 2. 3D-printed polypropylene flow cell used for temperature dependent experiments with forced flow. Invisible in this figure is the diaphragm, which is sandwiched between the two EPDM gaskets.

The cell was connected to the jacketed glass gas-liquid separators using C-flex Ultra Masterflex tubing. The outer jacket of the gas-liquid separators was connected to a thermostat (Brinkmann MGW Lauda C6 and Brinkmann MGW Lauda R22; CS control units) to allow for temperature control of the electrolyte. Throughout all the experiments, the gas-liquid separators were flushed with  $\text{N}_2$ . The separated gases were led to cooling columns to condense evaporated water and finally passed through gas scrubbers to clean off residual KOH. The catholyte and anolyte streams were then mixed with each other before entering the pump (Allied Motion, Bedu Pompen, flow rate = 9 mL/s; residence time per half-cell = 1.5 s) and led back to the electrolysis cell. A thermocouple was located before the cell inlet to monitor the electrolyte temperature via the potentiostat. The thermostat temperature was set to 20, 50, and 85 °C leading to cell inlet temperatures of  $22.2 \pm 1.3$ ,  $51.5 \pm 1.3$ , and  $74.8 \pm 1.5$  °C.

The exsolution CCDs were tested against a benchmark with pristine Zirfon and Ni felts as well as a well performing conventional catalyst CCD with Raney Ni for the HER and FeNi LDH for the OER. From the polarization curves in Figure 3, we can clearly observe that the exsolution CCD does not perform better than the benchmark, rather it resembles the curve shape of the benchmark precisely at both 20 and 80 °C. The poor performance might have been arising due to bad electrical contact between the PTL and the exsolution catalyst particles. We tried to solve this problem by adding a surplus of graphitized carbon to the ink mixture, as we have performed studies with Pt loaded on

graphitized carbon before that yielded some performance improvements. However, as clearly indicated by the polarization curves this did not help to improve the performance. We can generally observe in the kinetically controlled region between 2 and 100 mA/cm<sup>2</sup>, however, that there is a slight reduction between the CCDs with exsolution catalysts and the Ni felt benchmark.

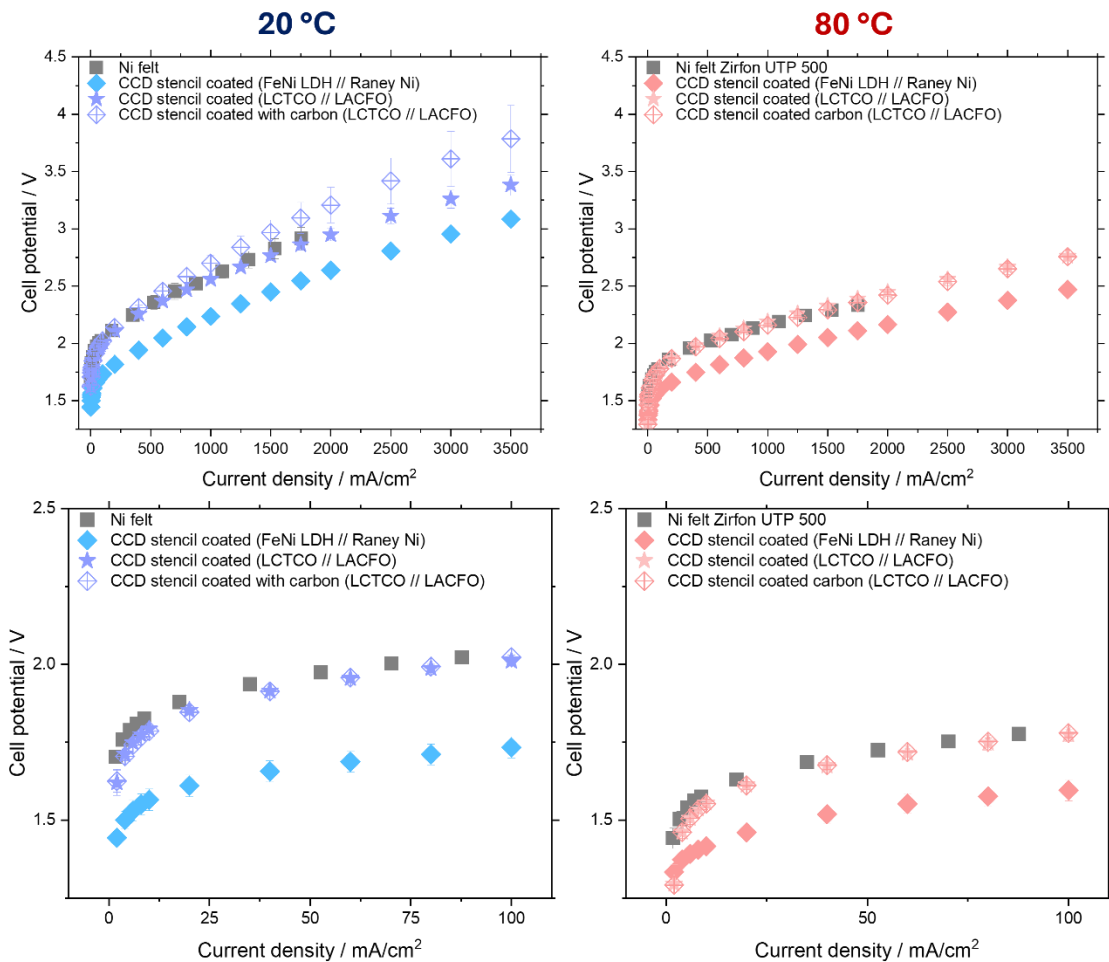


Figure 3. Polarization curves of pristine Zirfon with Ni felts, exsolution CCDs, and a conventional CCD. The measurements were conducted in 30 wt.% KOH with 50  $\mu$ M electrolyte Fe.

When we compare the internal resistance corrected polarization curves with each other, we can evidently see that the electrochemical kinetics between the benchmark and the exsolution CCDs are almost the same. This indicated that a CCD with exsolution catalysts is intrinsically more active than a pure Ni felt, however, the ceramics that serve as the support of the exsolution catalysts

seem to add extra resistances leading to an increase in Tafel slope and lower performances, especially at higher current densities.

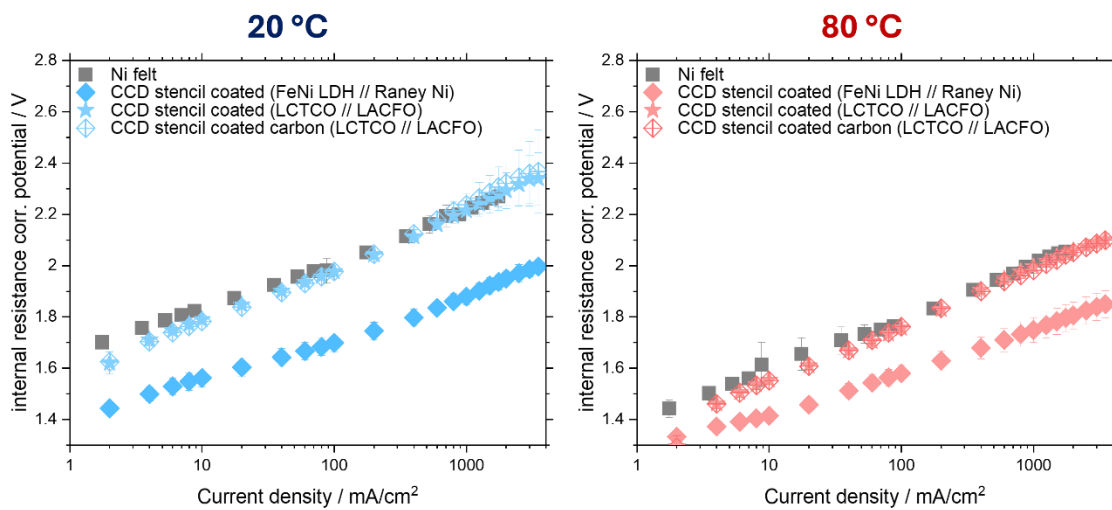
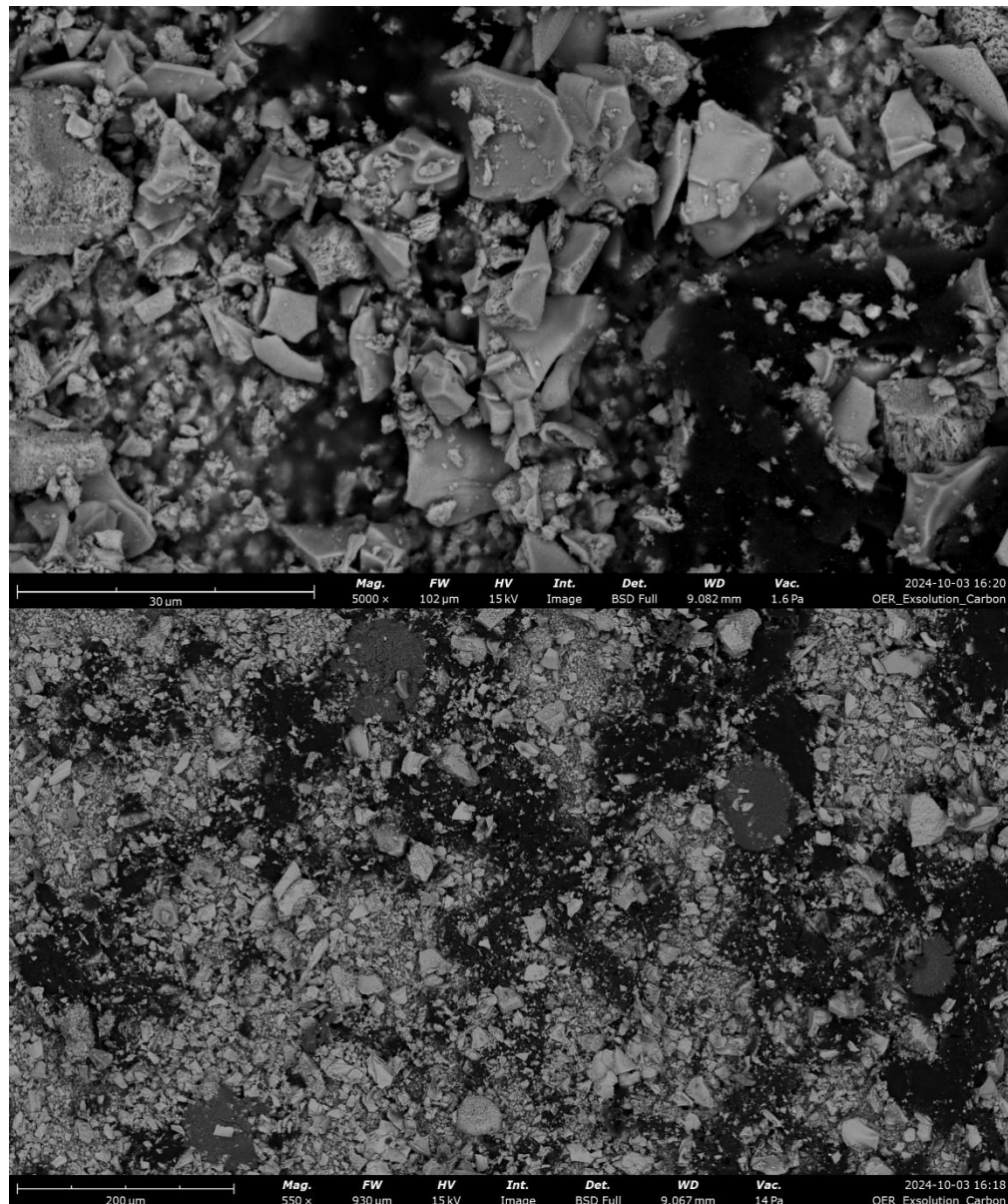


Figure 4. Internal resistance corrected polarization curves of pristine Zirfon with Ni felts, exsolution CCDs, and a conventional CCD. The measurements were conducted in 30 wt.% KOH with 50  $\mu$ M electrolyte Fe.

While the CCD were not stable over the course of the entire experiment, we could still observe that sufficient catalyst remained in the CCD/PTL interlayer to theoretically promote both HER and OER kinetics.



Element Symbol	Wt.%
C	25.600
O	34.900
K	5.900
Ca	8.000
Ti	16.900
Co	2.500
Zr	6.200

Figure 5. SEM images of the exsolution catalyst (Co-doped titanate) combined with graphitized carbon at varying resolutions. The table gives information about the elemental composition derived from EDX measurements.

Post electrolysis we have also investigated the CCDs concerning stability and we found that most of the catalyst remained on the surface of the CCD and is well intermixed with the carbon. We noticed that the catalyst formed small platelets in the sub 10  $\mu\text{m}$  range, however, this should not lead to a significant loss in conductivity. From the elemental analysis via EDX we could confirm that the main constituents that make up the exsolution catalysts (Ca, O, Ti, Zr, Co) is present on the surface. Therefore, we can conclude that the exsolution CCD was stable enough to be measured post electrolysis and thus the poor electrochemical activity does not arise from the instability of the exsolution CCD, but rather a poor electrical contact between the PTL and the catalytic particles.

From TEM images in Figure 6 we could observe that exsolution was prominent on the Co-doped titanate and also occurred on the Fe,Co-doped aluminate. As such those particles should inherently be electrochemically active if reached by a sufficiently high electrochemical potential.

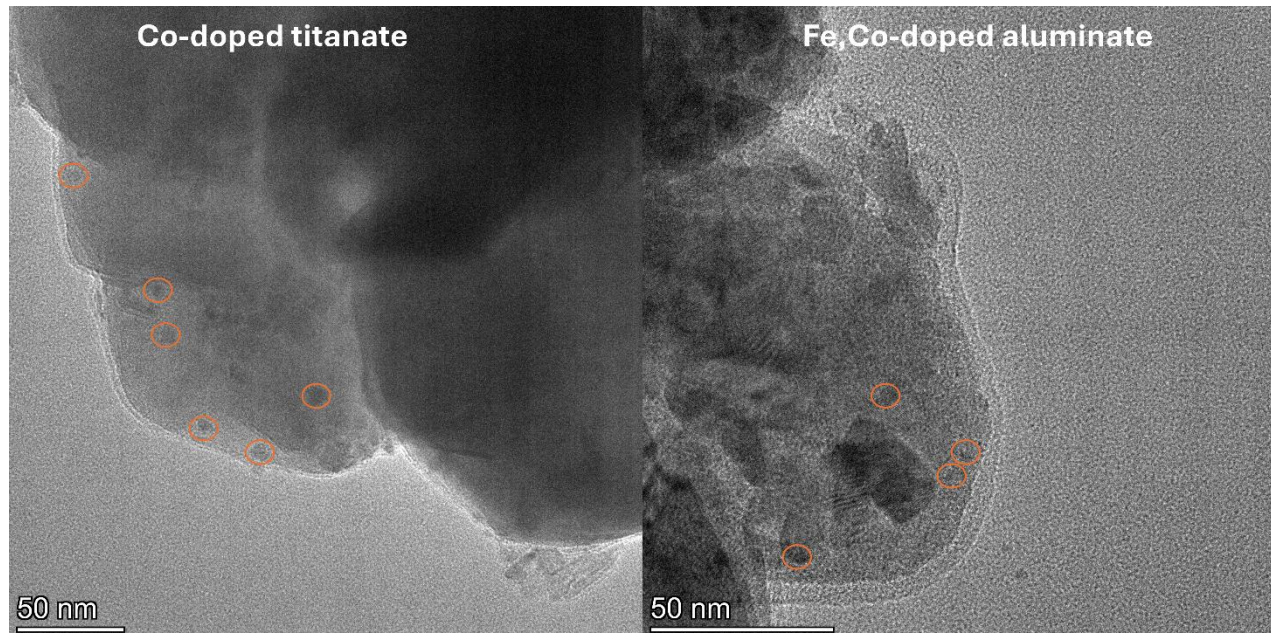


Figure 6. TEM images of Co-doped titanate and Fe,Co-doped aluminate showing exsolution on the surface.

### 3 Deviations

The results deviate from the expected outcome that the exsolution catalyst should improve the performance by a significant amount, while we only saw slight improvements at low current densities. In feedback with the partners in Work Package 1 we concluded that creating a good electrical contact between the current delivering/collecting PTL is challenging and not as straightforward as for conventional catalysts. Especially at high current densities, the conductivity seems to be limited. While measurements are being performed by Work Package 1 for the application of exsolution CCS, the measurements are not yet completed. Thus, a comparison between CCS and CCD cannot be shown. If well connected to the PTL, the CCS approach should lead to a better transfer of the electrochemical potential to the catalyst layer. In combination with an improved conductivity of the exsolved catalyst powder, this may further improve polarization curves in upcoming project phases. Thus, if the CCS manages to lead to a significant reduction in potential versus a non-coated benchmark, this will prove already that the CCS approach is better suited than the CCD approach for this kind of exsolution catalysts.

### 4 Conclusions

As the usage of exsolution CCDs did not yield better results than conventional CCDs, the upscaling in WP3 task 3.4 will be performed with conventional catalysts. While exsolution catalysts might be a promising approach for CCS, the conductivity needs to be improved to a level that is similar to Raney Ni particles. Then an application using CCD might be feasible as well. Alternatively, a combination approach for CCS and CCD is feasible, there the optimal coating choice is chosen based on the best performance results for both HER and OER.